YMTHE, Volume *28*

Supplemental Information

CAR T Cells Targeting MISIIR for the Treatment of Ovarian Cancer and Other Gynecologic Malignancies

Alba Rodriguez-Garcia, Prannda Sharma, Mathilde Poussin, Alina C. Boesteanu, Nicholas G. Minutolo, Sarah B. Gitto, Dalia K. Omran, Matthew K. Robinson, Gregory P. Adams, Fiona Simpkins, and Daniel J. Powell Jr.

SUPPLEMENTAL FIGURES

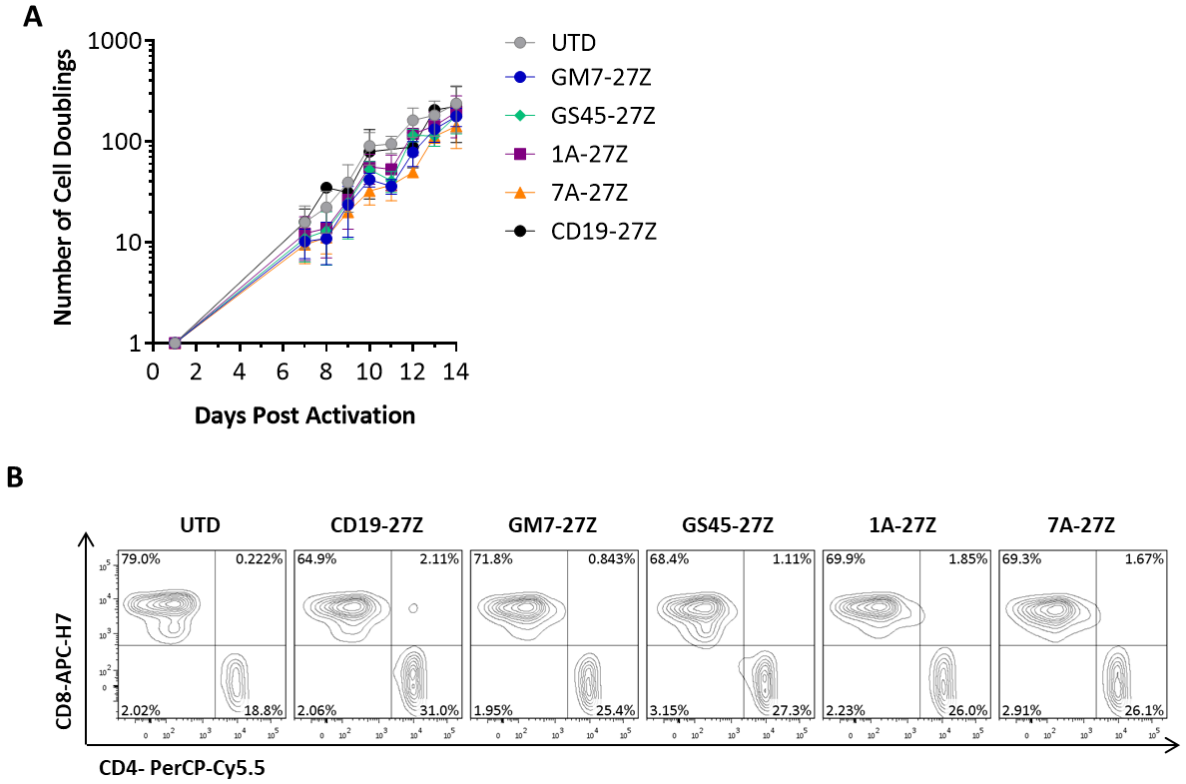

Figure S1. MISIIR CAR T-cell variants show a similar *in vitro* expansion and CD4/CD8 ratio. (A) Number of cell doublings during a period of 14 days after activation with CD3/CD28 beads is shown. Combined data from 6 donors is represented as mean ± SD. (B) T-cells were stained at day 14 post-activation for CD4 (X-axis) and CD8 (Y-axis). Cells were previously gated on live/CD3^{+}. Data from one representative donor is represented.

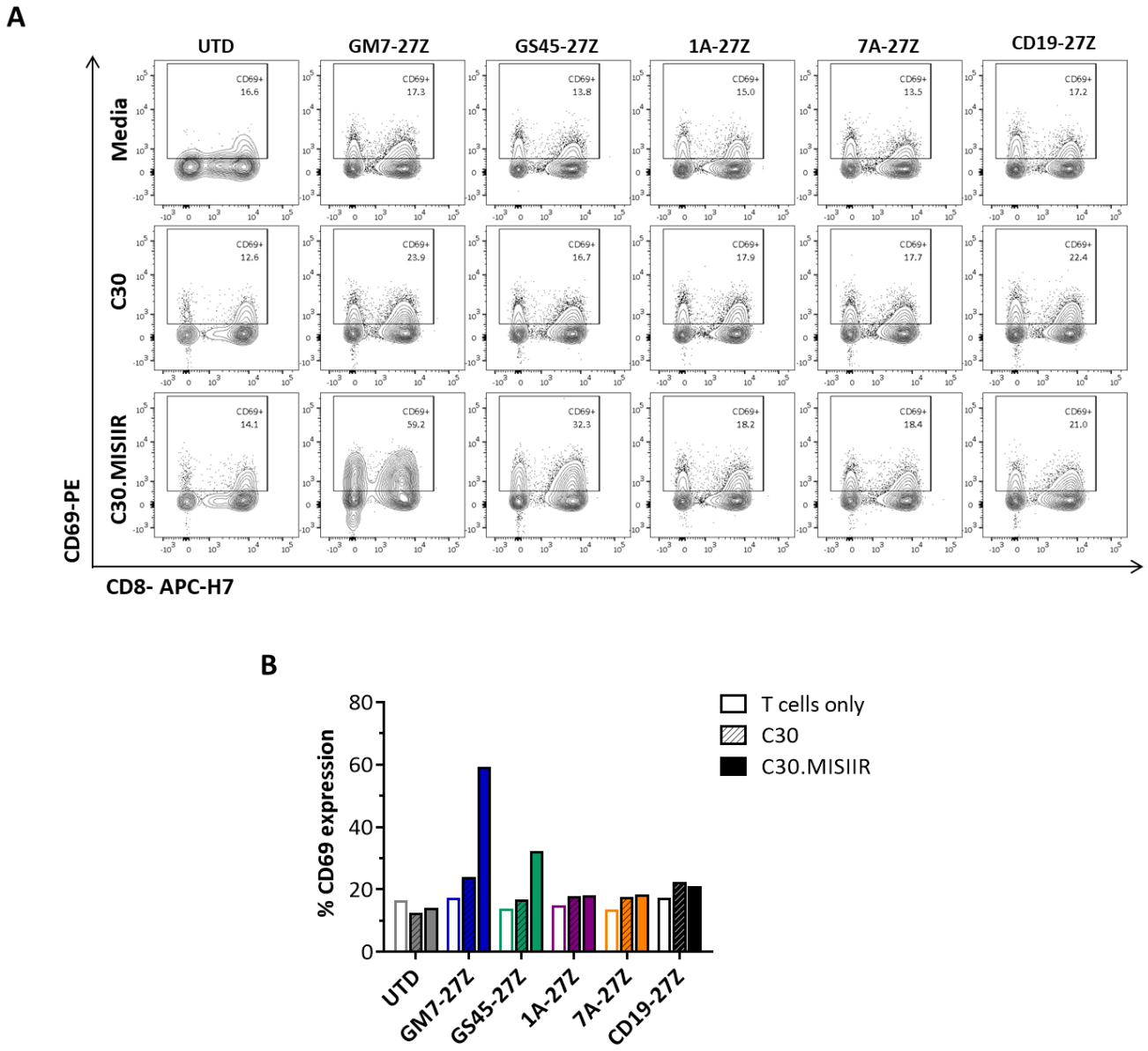

Figure S2. GM7 and GS45 CAR T-cells upregulate CD69 in co-culture with C30.MISIIR target cells. Co-cultures of the distinct MISIIR CAR T-cells variants and C30 or C30.MISIIR were established at 1:1 E:T ratio. (A) CD69 upregulation after 24 hours of co-culture was assessed. CD69 (Y-Axis) versus CD8 (X-Axis) is represented for live/CD3$^+$ gated cells. (B) Quantification of CD69 expression in live/CD3$^+$ cells represented as frequency.

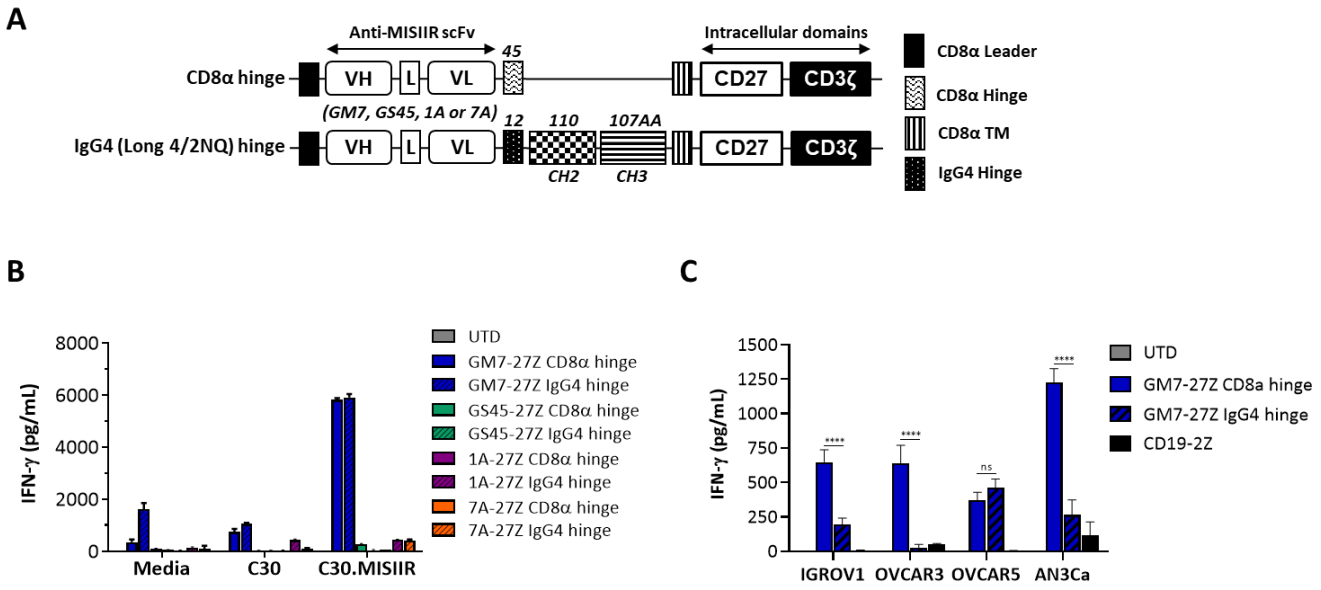

Figure S3. Replacement of CD8a hinge by a longer IgG4-based hinge does not rescue reactivity in any of the MISIIR CAR variants. (A) Schematic representation of CAR constructs including the CD8a hinge or the IgG4 (long 4/2NQ hinge). (B) IFN-γ concentration as detected by ELISA in 24-hour supernatants from co-cultures of the CAR T-cells including both hinges and C30/C30.MISIIR target cells. (C) IFN-γ concentration as detected by ELISA in 24-hour supernatants from co-cultures of GM7 CAR T-cells including both hinges and tumor cell lines expressing endogenous levels of MISIIR. Data is represented as mean ± SD.

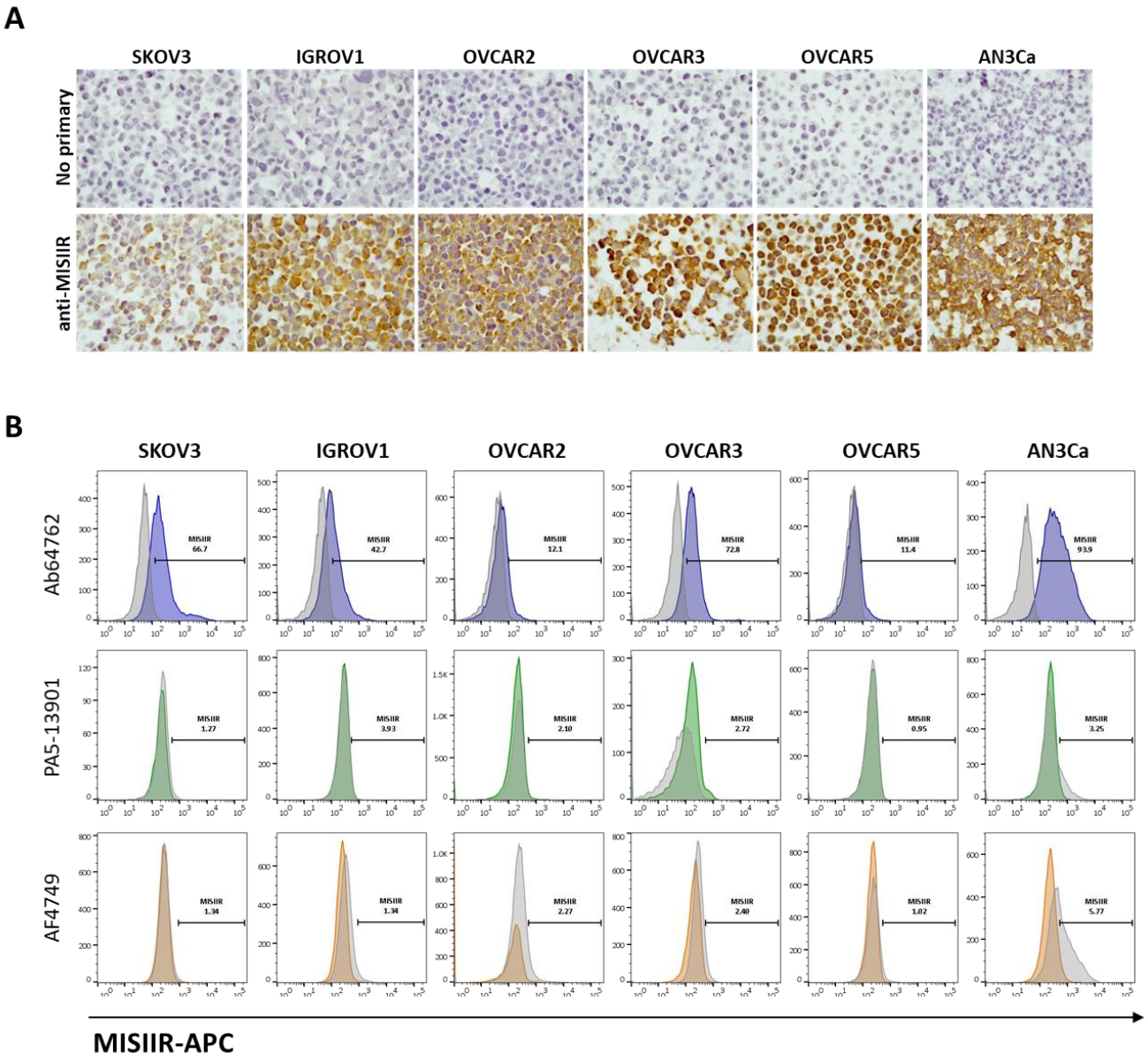

Figure S4. MISIIR is expressed in ovarian and endometrial cancer cell lines. Endogenous levels of MISIIR expression in a panel of human ovarian (SKOV3, IGROV1, OVCAR2, OVCAR3, and OVCAR5) and endometrial (AN3Ca) cancer cell lines as assessed by (A) IHC staining (upper panel shows negative control in the absence of primary antibody) or by (B) flow cytometry.

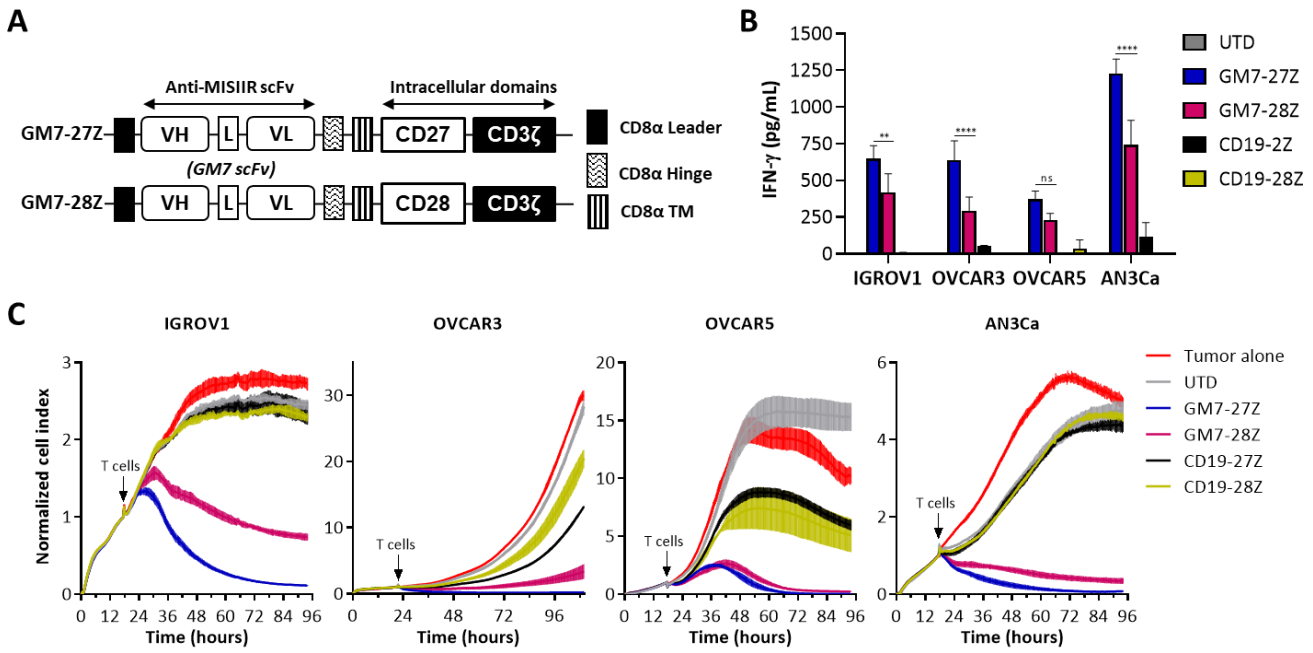

Figure S5. CD27 co-stimulated GM7 CAR construct secretes higher IFN-γ levels and possess faster killing kinetics than CD28 counterpart in co-culture with MISIIR-expressing tumor cells. (A) Schematic representation of GM7 CAR constructs including the CD27 or CD28 co-stimulatory domains. (B) Antigen-specific IFN-γ production by CD27 or CD28 co-stimulated CAR T-cells as detected by ELISA from 24-hour co-culture supernatants. Co-cultures were established at a 1:1 E:T ratio. Significance was determined by two-way ANOVA and Dunnett's multiple comparison test as compared to UTD group. **** $p<0.0001$; ** $p<0.01$. (C) Real-time cytotoxicity assays established at a 3:1 E:T ratio. Data is represented as mean ± SD. Arrows indicate time of CAR T-cell addition.

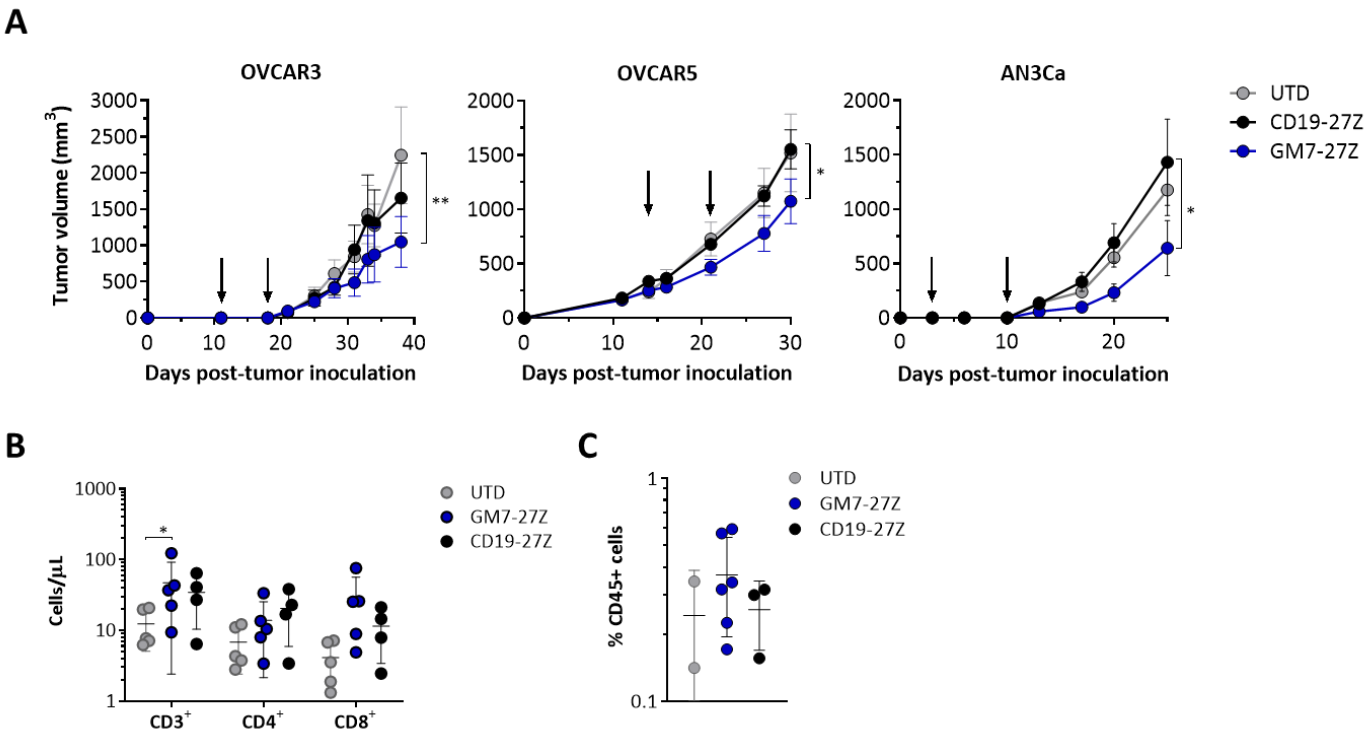

Figure S6. GM7 CAR T-cells demonstrate antigen-specific reactivity against endogenous MISIIR *in vivo*. (A) OVCAR3, OVCAR5 or AN3Ca GFP-fLuc cells were inoculated into NSG mice subcutaneously. Once the tumors were established, mice were randomized in groups and received two intravenous doses of CAR^+ T-cells ($5x10^6$) given one week apart. Tumor growth was monitored by caliper measurement. Arrows indicate times of T-cell administration. Data is represented as mean ± SD. Significance was determined by two-way ANOVA and Tukey's multiple comparison test. * $p<0.05$, ** $p<0.01$. (B) Absolute numbers of human $CD3^+$, $CD4^+$, and $CD8^+$ T-cells as quantified by flow cytometry on day 18 post-T cell injection for the AN3Ca model. Data is represented as mean ± SD. Significance was determined by two-way ANOVA and Tukey's multiple comparison test. * $p<0.05$. (C) Frequency of $CD45^+$ cells in tumor digests at the endpoint of the AN3Ca study.

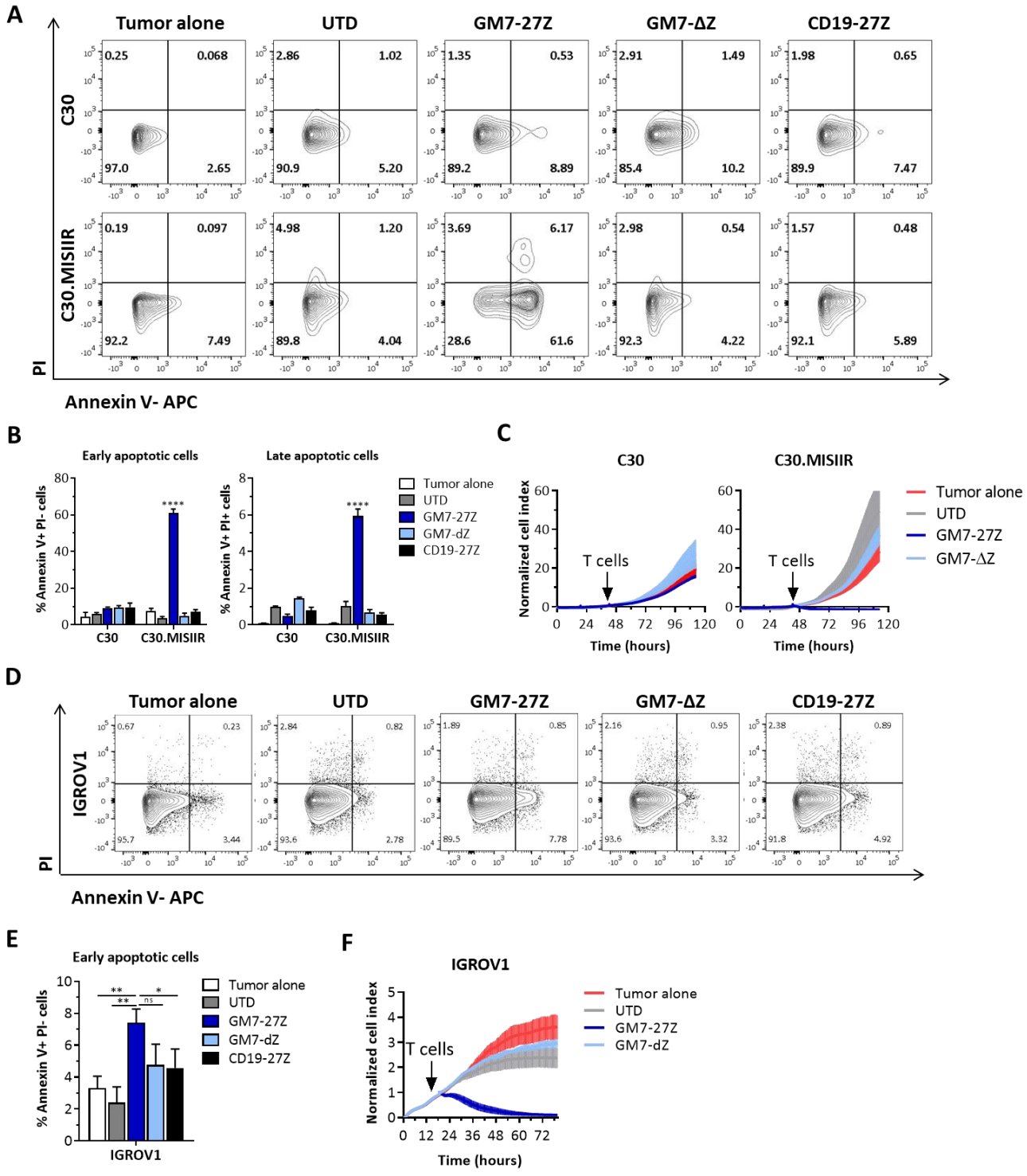

Figure S7. GM7 CAR T-cells killing mechanism does not involve ligand-induced apoptosis. (A) Representative flow plots of the staining of the apoptotic markers Annexin V (X-axis) and PI (Y-axis) after 24 hours of co-culture with C30 or C30.MISIIR target cells at 1:1 E:T ratio. (B) Frequency of early (Annexin V^+ PI^-) and late (Annexin V^+ PI^+) apoptotic cells. (C) Real-time cytotoxicity assays established at a 1:1 E:T ratio. (D) Representative flow plots of the staining of the apoptotic markers Annexin V (X-axis) and PI (Y-axis) after 48 hours of co-culture with IGROV1 target cells at 3:1 E:T ratio. (E)

Frequency of early (Annexin V^+ PI^-) apoptotic cells. (F) Real-time cytotoxicity assays established at a 3:1 E:T ratio. Data is represented as mean ± SD. Significance was determined by two-way ANOVA and Dunnett's multiple comparison test as compared to UTD group. **** $p<0.0001$; ** $p<0.001$; * $p<0.05$.

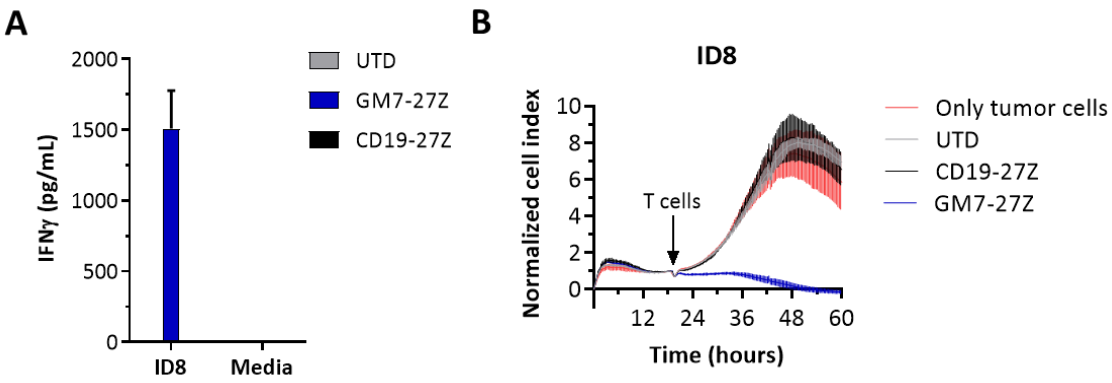

Figure S8. GM7-27Z CAR cross-reacts with mouse MISIIR protein. (A) Antigen-specific IFN-γ production by GM7 CAR T-cells as detected by ELISA from 24 hour supernatants from co-cultures with ID8 mouse ovarian cancer cell line. Co-cultures were established at a 1:1 E:T ratio. (B) Real-time cytotoxicity assays established at a 3:1 E:T ratio. Data is represented as mean ± SD.

SUPPLEMENTAL METHODS

Construction of anti-MISIIR GM7 CAR with CD28 costimulatory domain. Plasmid encoding GM7 scFv was obtained and amplified by PCR as specified in Materials and Methods section. The PCR product was digested and ligated into previously described third-generation pELNS lentiviral vectors containing CD28-CD3Z signaling domains [1] .

Construction of anti-MISIIR CARs with IgG4 (long 4/2NQ hinge). A DNA vector encoding for the IgG4-based hinge long 4/2NQ [2], CD8 TM domain, CD27 and CD3ζ flanked by NheI and SalI restriction sites was synthetized by Integrated DNA Technologies, Inc. (IDT). The fragment was then digested and ligated into previously described pELNS lentiviral vectors containing anti-MISIIR scFvs.

Immunohistochemistry. IHC for MISIIR was performed in formalin-fixed, paraffin-embedded tumor cell pellets. Sections were deparaffinized according to standard IHC protocols. Heat-induced epitope retrieval was performed using pH6 Citrate buffer (Thermo). Staining was performed using Cell & Tissue Staining Kit HRP-DAB system anti-sheep (R&D Systems, cat. #CTS019) according to the manufacturer's instructions. Primary human MISIIR antibody (R&D Systems, cat. #AF4749) was used at 10µg/mL and incubated for 1 hour at room temperature. Slides were counterstained with hematoxylin, dehydrated and mounted. 40X pictures were captured on a NikonXMZ microscope.

MIISIR surface expression. The following antibodies: Ab64762 (Abcam), PA5-13901 (Thermo Fisher), and AF4749 (R&D Systems) were conjugated with APC using the Lightning-Link APC antibody labeling kit (Novus Biologicals) according to manufacturer's instructions, and used to stain for surface MISIIR in tumor cell lines.

***In vivo* studies**. Peripheral blood sampling was conducted via retro-orbital blood collection under isoflurane anesthesia. In all, 50 µL blood was labeled for the indicated cell markers and quantified using TRUCount beads (BD Biosciences). Tumors were collected at the endpoint of in vivo studies, dissociated into single cell suspensions using GentleMACS technology, and stained for flow cytometry as described in Materials and Methods.

SUPPLEMENTAL REFERENCES

1. Lanitis, E., et al., *Redirected antitumor activity of primary human lymphocytes transduced with a fully human anti-mesothelin chimeric receptor.* Mol Ther, 2012. **20**(3): p. 633-43.
2. Hudecek, M., et al., *Receptor affinity and extracellular domain modifications affect tumor recognition by ROR1-specific chimeric antigen receptor T cells.* Clin Cancer Res, 2013. **19**(12): p. 3153-64.